ECOLOGY

The balance of dissolved oxygen and pH levels is paramount in aquaculture, as a media for cultivating aquatic organisms under controlled conditions. An imbalance in both oxygen and pH could severely harm the cultured aquatic organisms. Various strategies are used to prevent hypoxia and maintain the pH level of the culture. Interestingly, hypoxia or deprivation of oxygen supply in aquaculture was often reported to co-occur with the seawater acidification. Despite that, there was no evidence that the O_2 level was directly linked to pH changes. Thus, the existing treatment strategies are separated between O_2 and pH maintenances, which often inflate cost and cause environmental burden due to the use of synthetic chemicals. This study was conducted to observe the mechanism and effect of the O_2 addition to aquaculture seawater in molecular level when the pH value of the water was modified. The understanding of the mechanism may lead to an alternative to the harmful aquaculture treatments. The molecular mechanics analysis was applied to examine the mechanism of pH adjustment in non-aerated and aerated seawater. The results indicated that O_2 accelerated the pH recalibration of seawater, particularly in the alkaline modified samples compared to the acid modified samples. Mechanical simulations further showed the repulsion between CO_3^{2-} and O_2 causes vibration which shortens OH bond by 17.71 % while elongates O-O bond by 1.00 %. Additionally, the spin coupling between OH- and O_2 promotes global energy transfer which stimulates the vibration of the alkaline modified water system. Together, those mechanisms enabled the pH value to return to the baseline. These findings contribute a molecular mechanism view of aquaculture pH maintenance in the presence of O_2, as well as revisiting the use of aeration in aquaculture treatment

Keywords: aeration treatment, molecular mechanism, dissolved oxygen, pH recalibration, aquaculture seawater

UDC 613
DOI: 10.15587/1729-4061.2022.266012

THE MECHANISM OF pH RECALIBRATION BY DISSOLVED OXYGEN IN ALKALINE MODIFIED AQUACULTURE SEAWATER

Wresti L. Anggayasti
Corresponding author
Doctor of Philosophy, Assistant Professor*
Postgraduate School of Brawijaya University**
E-mail: wl.anggayasti@ub.ac.id
Willy Satrio N.
Doctor (Mechanical Engineering)
Department of Industrial Engineering**
I Nyoman Gede Wardana
Doctor of Philosophy, Professor*
Andi Kurniawan
Doctor of Science, Associate Professor
Department of Aquatic Resources Management**
*Department of Mechanical Engineering**
**Brawijaya University
Jl. Veteran, 1, Malang, East Java, Indonesia, 65145

Received date 11.08.2022
Accepted date 13.10.2022
Published date 28.10.2022

How to Cite: *Anggayasti, W. L., Satrio N., W., Wardana, I. N. G., Kurniawan, A. (2022). The mechanism of pH recalibration by dissolved oxygen in alkaline modified aquaculture seawater. Eastern-European Journal of Enterprise Technologies, 5 (10 (119)), 6–13. doi: https://doi.org/10.15587/1729-4061.2022.266012*

1. Introduction

The potential of aquaculture in supplying the demand of seafood consumption and export in Indonesia has risen dramatically within the past decade. Although the rapid growth of aquaculture industry for providing food products raised concerns for environment sustainability [1], aquaculture itself can be utilized to restore habitats and potentially rebuild populations of rare and endangered water species [2]. As its name implied, aquaculture is a cultivation system with controlled parameters, among others are oxygen and pH. Any disturbances towards those parameters could lead to severe damages to the culture ecosystems. Therefore, carefully managed maintenance to preserve the parameters' balance is important. However, to date, the maintenance of pH and oxygen levels mostly relied on the use of chemicals which do not support environment sustainability. This research on the relationship between mechanisms of aeration, which ensures the oxygen supply for aquaculture, and pH level maintenances thus becomes relevant for consideration of a more affordable and environmentally friendly maintenance system.

2. Literature review and problem statement

Previous paper [3] elaborated that dissolved oxygen (DO) level is a crucial factor in aquaculture. It is shown that the condition of low DO, or hypoxia, was proven to be life threatening to the cultivated aquatic organism, for example, the white leg shrimp or *Litopenaeus vannamei* [3]. This white leg shrimp rapid reproduction is highly beneficial, thus making it a profitable food commodity. However, because of the rapid population growth, the competition for oxygen supply in the ecosystem is increasing overtime [3]. These results in low DO condition. Another problem that may arise from this situation is the possibility of increasing impurities in the water [4]. Those findings demonstrated

that low DO is an enormous threat for the biotic components in the marine ecosystems. It is the root cause of any physiological problem of *L. vannamei* and many other aquatic ecosystems or biotic components.

The most concerning side effect of lower O_2 in a densely populated marine ecosystem is the increase of CO_2 [5]. The effect of rising CO_2 in the water generates a cycle that increases the overall temperature in the water itself and around the water. The cycle occurs due to the released CO_2 from the water on the surface that immediately reacts with the surrounding air [6]. As a result, the air temperature around and inside the water got simultaneously higher. The prolonged corresponding condition may cause the biotic components to experience hyperthermia. The *L. vannamei* may survive from hyperthermia through heat shock protein (HSP) 70 and HSP90 modification. A couple of HSP proteins including HSP70 are also known to be involved as stabilizer in stress responses towards inflammatory diseases [7]. However, these HSP genes expressions in *L. vannamei* are decreasing during hypoxia [8], which could weaken the organism's ability to survive. It can be concluded that the DO level control is the most influential factor in aquaculture organism survivability. As such, the practice of aeration is very useful for aquaculture to ensure the presence of oxygen that has been proven to improve not only the aquaculture water quality, but also the growth and yield of aquacultural species [9, 10].

The other pivotal factor in aquaculture maintenance is pH stability, especially that some aquaculture uses seawater. The recent phenomenon of increasing acidity of global seawater, or ocean acidification, is known to negatively impact various biological functions of marine life and disrupt the stability of the global marine ecosystems [11]. Acidic water pH is also closely related to the emergence of various pathogenic microbes that cause disease in cultured organisms [12]. Interestingly, in aquaculture, the event of hypoxia was often accompanied by pH changes [11, 13]. However, despite the frequently reported co-occurrence of DO and pH deviations and its detrimental effects, there seems to be little to no evidence that those two factors are directly related. In practice, the pH maintenance in aquaculture is usually done separately from aeration.

An option to overcome the maintenance of pH and oxygen level is considering novel techniques that are exclusively developed to solve specialized problems in pH maintenance. For example, the coastal ecosystem seawater pH variability control based on nutrition was focused on the management of driver factors that consist of nutrients, organic matter, and alkalinity [14]. Another technique is using genetically modified *Bacilli* that also alter other water quality parameters such as conductivity, dissolved chemicals, and water physical properties [15]. The more sophisticated technique is through an automated intelligent system with Internet of things (IoT) control to pour the necessary chemicals at a certain time [16]. However, although those techniques increase the efficiency in aquaculture pH maintenance, the validation of the existing pH maintenance technique should be prioritized before developing the corresponding technology. Furthermore, the use of chemical for treatments even increases costs and burdens the environment. All this allows to argue that it is appropriate to conduct a study devoted to the investigation of the mechanism of the pH changes regulation by dissolved oxygen from aeration to the *L. vannamei* aquaculture seawater.

3. The aim and objectives of the study

The aim of this study is to evaluate the potential mechanism of pH maintenance with aeration to gain insights based on the fundamental chemical physics.

To achieve this aim, the following objectives are accomplished:

– to observe the pH status in non-aerated and aerated aquaculture seawater, both acid- and alkaline-modified, over 7 days;

– to employ molecular mechanics analysis to observe pH recalibration mechanism in non-aerated and aerated seawater systems;

– to implement the self-propelling algorithm with mean-field particle simulation to confirm the results of the molecular system analysis. This would support whether oxygen played a role in pH recalibration.

4. Materials and methods

Seawater used as a water source in *L. vannamei* culture (salinity of 30 ppt and pH 9.2) was chosen as the object of this study. The seawater is taken directly from the south coast of Malang Regency, East Java, Indonesia. It was modified by adding HCl 0.1 M for an acidic pH value of 6.1, and NaOH 0.1 M for an alkaline pH value of 11.2. To observe whether the addition of O_2 affected the pH of seawater, moderate aeration was introduced to a separate the set of samples. The changes of pH were monitored for seven days at ambient temperature, counting the day of pH modification as the first day. The underlying molecular mechanism was investigated by simulations using Avogadro (ver. 1.2.0) with Universal Force Field (UFF). The natural pH buffering capacity of seawater is regulated by its dissolved inorganic carbons (DIC). During simulation, the predominant DIC species was assumed to be CO_3^{2-} at all conditions, since the natural pH of the sample water was alkaline. The energy of the stabilized conformation and bond length changes were observed.

The molecular simulation results were confirmed through the mean-field particle simulation of the water system using Python programming language with SiSyPHE library [17]. The algorithm used was self-propelling algorithm which assumed that each particle is moving with the speed as specified in equation (1) [18]. The molecular interaction was controlled by the Morse potential as shown in equation (2).

$$\left(dV_t^i\right)/dt=\left(\alpha-\beta\left|V_t^i\right|^2\right)V_t^i- \\ -m/N\nabla_{(X^i)}\Sigma_{(j\neq i)}U\left(\left|X_t^i-X_t^j\right|\right), \quad (1)$$

$$U(r)=-C_a e^{-r/l_a}+C_r e^{-r/l_r}. \quad (2)$$

The interaction was simulated for 10000 particles (N) placed in random positions (X) with molecular masses of the contributing atoms as the particle mass (m). Each particle propulsion acceleration (α) and friction (β) was set to 1.6 and 0.5, respectively.

5. Results: Aeration Assists pH Recalibration of Alkaline-Modified Seawater

5. 1. pH status and simulation of acid-modified seawater

The results showed that acid-modified water reached a plateau of pH 8.3 on the fourth day (Fig. 1). Interestingly, the pH reactions of aerated seawater equilibrated faster, which indicated the contribution of O_2 towards pH regulation. In this case, the plateau pH of about 8.7 of the acid-modified water was reached on the second day, which carried on until day 7 (Fig. 1). The molecular simulation results further clarified the role of O_2. In acid-modified seawater, the molecules reacting with CO_3^{2-} are H^+, and Cl^-, assuming HCl dissociates completely into H^+ and Cl^- upon addition to water. Molecular simulation demonstrated that CO_3^{2-} got closer to both H^+ and Cl^- ions, as can be seen in Fig. 2, *c*, *d*, relative to the initial position in Fig. 2, *a*, *b*. The result described the natural buffering activity.

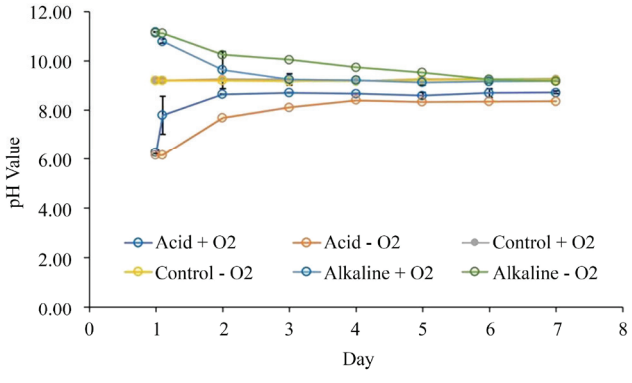

Fig. 1. The daily pH changes of acid and alkaline modified seawater, with and without aeration (O_2)

The general model of the pH daily rate of change was defined geometrically through the integration of the area under the curve in Fig. 1. The vertical axis represents the pH value while the horizontal axis represents the time evolution in day. Hence, the x symbol represents the day and the y symbol represents pH value. Since the pH value changed every day, the continuity assumption is acceptable to assemble the model. Based on the visual representation, the variable interrelationship is linear. The changes of the pH value were never higher than the maximum pH value of *h* and never lower than the lowest pH value of *l*. Both, acid-initial or alkaline-initial solution always return the final pH in neutral region. The rate of change of the pH value is depends on the time evolution dependent variable of *x*. Therefore, the total pH change by taking the account of continuity is the expansion progression of the area under the curve as shown by the integral formula with a general form as in equation (3).

$$y=\int_l^h f(x)\mathrm{d}x. \tag{3}$$

Equation (4) is Given by,

$$y=\int_l^h (x+xdx)\mathrm{d}x, \tag{4}$$

where x – day, y – pH value.

Let dx – daily rate of change of the pH value, l – lowest pH value, h – highest pH value, then xdx – progression of the daily pH evolution.

The general model of the pH daily rate of change was defined geometrically through the integration of the area under the curve in Fig. 1. The vertical axis represents the pH value while the horizontal axis represents the time evolution in day. Hence, the x symbol represents the day and the y symbol represents pH value. Since the pH value changed every day, the continuity assumption is acceptable to assemble the model. Based on the visual representation, the variable interrelationship is linear. The changes of the pH value were never higher than the maximum pH value of *h* and never lower than the lowest pH value of *l*. Both, acid-initial or alkaline-initial solution always return the final pH in neutral region. The rate of change of the pH value is depends on the time evolution dependent variable of *x*. Therefore, the total pH change by taking the account of continuity is the integral formula as shown in equation (3).

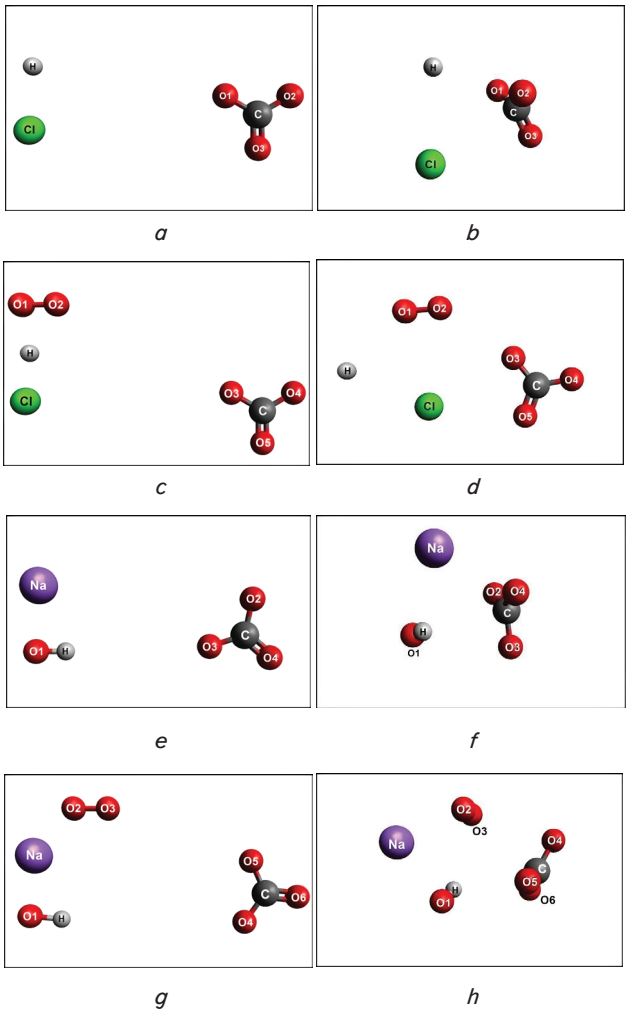

Fig. 2. The molecular simulation of acid-modified seawater: *a* – without O_2 before and *b* – after simulation; *c* – with O_2 before and *d* – after simulation; the molecular simulation of alkaline-modified seawater: *e* – without O_2 before and *f* – after simulation; *g* – with O_2 before and *h* – after simulation

When O_2 was added, the reaction stabilized quicker. The O_2 occupied nearer position to CO_3^{2-} and Cl^-, while the H^+ located further away (Fig. 2, *d*). This suggested that H^+ was

more unlikely to bind the CO_3^{2-} ion and possibly caused the more acidic pH than the control pH 9.2. The overall energies of the reactions with and without O_2 were –3.95 and –3.07 kJ/mol, respectively. Both indicated endothermic bond formation. However, the ion interactions of the sample without O_2 may be weaker than with O_2. In other words, the H^+ in acid-modified seawater without aeration might interact more loosely with CO_3^{2-}, resulted in a lower pH.

5. 2. pH status and simulation of alkaline modified seawater

Meanwhile, the alkaline modified seawater stabilized at a pH of 9.2 on the sixth day, as shown in Fig. 1. Upon the addition of O_2, the alkaline modified water reached the plateau pH of 9.2 on the third day (Fig. 1). The process was faster than the acid-modified seawater, and in both non-aerated and aerated samples, the pH returned to the baseline of the control. In the molecular simulation of the alkaline modified seawater, the reacting ions are CO_3^{2-}, OH^-, and Na^+ if NaOH dissociates completely. The stable conformation showed that both OH^- and Na^+ moved closer to CO_3^{2-} (Fig. 2, *f*, compared to the initial position in Fig. 2, *e*).

Furthermore, the reaction stabilized faster upon the addition of O_2. The end position of the O_2 was closer to CO_3^{2-} and OH^- compared to Na^+ (Fig. 2, *h*, compared to the initial position in Fig. 2, *g*). Interestingly, in the stabilized conformation, the bonds within the OH^- ion were shortened by 17.71 % for the reaction with O_2 and 8.08 % for the reaction without O_2 (Table 1). On the other hand, the bond within O_2 stretched by 1 % (Table 1), and the overall energy changed from –2.72 kJ/mol without O_2 to –5.14 kJ/mol with O_2.

Further molecular simulation of alkaline seawater clarified the CO_3^{2-} role in pH reduction, as shown in Fig. 3. The presence of CO_3^{2-} in non-aerated seawater had aligned the water positive dipoles of the water molecules towards the CO_3^{2-} negative dipoles. The positive dipoles competed with sodium ions to create a bond with CO_3^{2-}. As a result, the carbon atom of CO_3^{2-} was destabilized and attracted another water molecule. This phenomenon is depicted in Fig. 3, *a* as the formation of a long green force vector from the C atom.

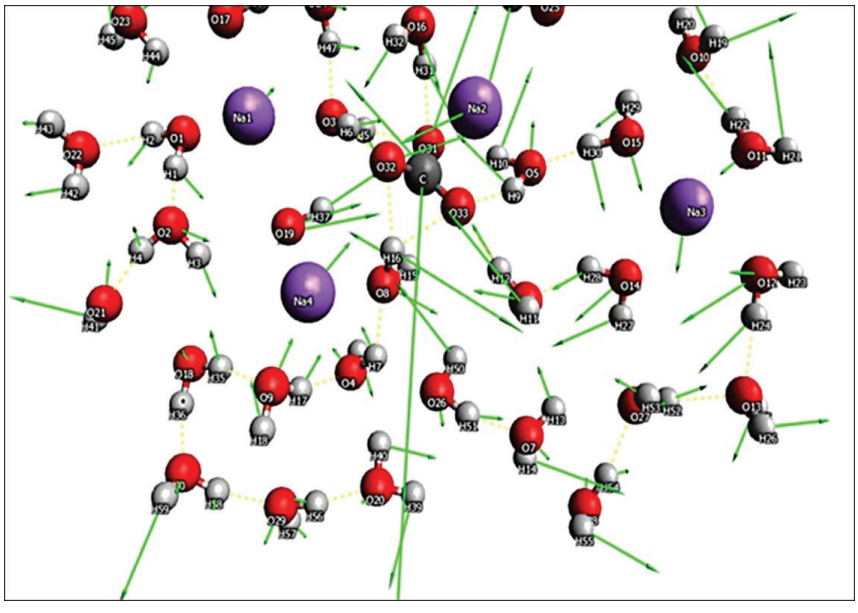

a

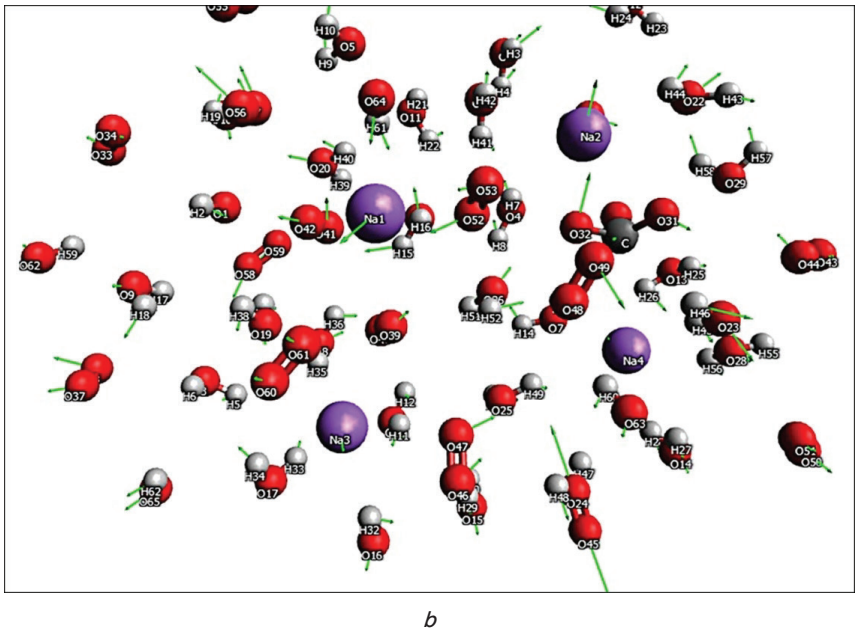

b

Fig. 3. The simulation of the CO_3 behaviour: *a* — in non-aerated alkaline water; *b* — in aerated alkaline water

However, the hydrogen bonds of the water molecules were uninterrupted (yellow lines in Fig. 3, *a*) despite the sodium ions promoting the ion cluster formation. Meanwhile, the aerated alkaline seawater forced CO_3^{2-} to vibrate. The vibration was the result of the continuous O_2 oxygen atom repulsion with C-O on CO_3^{2-}. The aerated alkaline seawater atoms condition is demonstrated in Fig. 3, *b*, with shorter green vector compared to the non-aerated atoms.

Table 1

The changes of bond length in alkaline modified seawater

Alkaline modified	Start atom	End atom	Bond length (Å)		Change (%)
			Before	After	
without O_2	O1	H	1.077	0.990	8.08 % shorter
with O_2	O1	H	1.203	0.990	17.71 % shorter
	O2	O3	1.303	1.316	1.00 % longer

5. 3. Mean-field particle simulation of the seawater system

The mean-field particle simulation validated the molecular dynamics simulation results and predicted the system behavior in high temperature. For Fig. 4, *a–c*, the parameters were *N*=10000, alpha=1.6, beta=0.5, Ca=1.0, la=2.75, Cr=1.0, and lr=1.84. Time courses for Fig. 4, *a–c*

were 0.0, 1.0, and 100.0, respectively. As for Fig. 4, *d–f*, the parameters were *N*=10000, alpha=1.6, beta=0.5, Ca=1.0, la=1.542, Cr=1.0, and lr=1.84. Whereas the time courses for Fig. 4, *d–f* were similar with those of Fig. 4, *a–c*. The six remaining figures (Fig. 4, *g–l*) had the same parameters with the first six ones, except for Fig. 4, *g–i*, la=2.5278 and for Fig. 4, *j–l*, la=1.542. The time courses were 0.0 for Fig. 4, *g, j*, 1.0 for Fig. 4, *h, k*, and 100.0 for Fig. 4, *i, l*. Those figures described that the simulated water system behavior was consistent with the molecular dynamics simulation results.

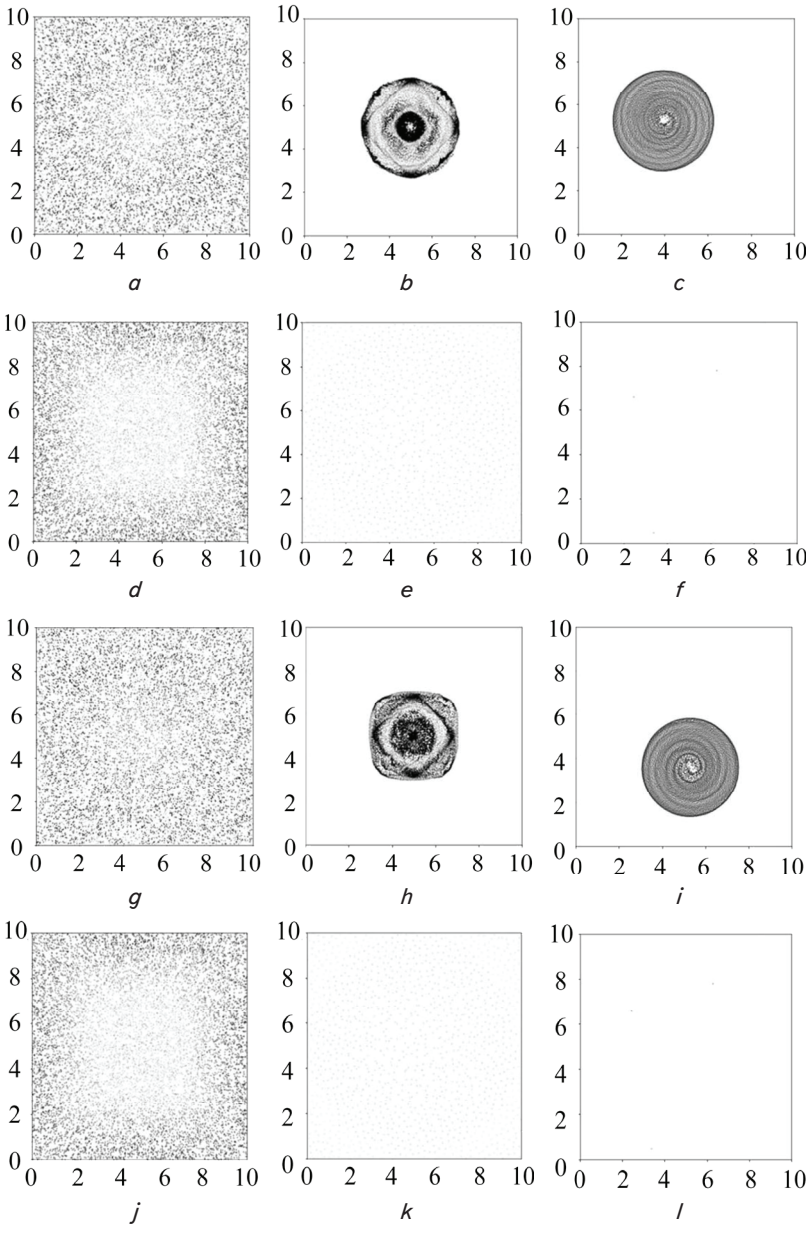

Fig. 4. Mean-field particle simulation results: *a* — of non-aerated initial condition; *b* — of non-aerated first frame; *c* — of non-aerated last frame; *d* — of aerated initial condition; *e* — of aerated first frame; *f* — of aerated last frame; *g* — of alkaline non-aerated initial condition; *h* — of alkaline non-aerated first frame; *i* — of alkaline non-aerated last frame; *j* — of alkaline aerated initial condition; *k* — of alkaline aerated first frame; *l* — of alkaline aerated last frame

Without aeration, it is possible for water molecules to form a group when each water molecule is propelled. This is depicted by the transition of Fig. 4, *a*, *b* where a spherical shape was formed. The last step of the simulation in Fig. 4, *c* showed that the interaction persisted as the size of the formed vortex was equal to the size of the sphere in Fig. 4, *b*. Meanwhile, the presence of O_2 prevented the water molecules to form a group as shown by the scattering trajectories in the transition of Fig. 4, *d, e*. The last step of the simulation showed vanishing vertices (Fig. 4, *f*) which indicated the prevention of hydrogen bond by nonpolar O_2.

The alkalization effect was undetected for non-aerated (Fig. 4, *g–i*) and aerated water (Fig. 4, *j–l*) as the formed trajectories patterns were similar. However, both Mean-field particle and molecular dynamics simulations revealed the O_2 role as the water molecule movement initiator.

6. Discussions: the mechanism of aeration in returning the modified pH to the baseline

As a discussion of the results of acid-modified seawater (Fig. 1), more specifically, the weaker ion interaction of non-aerated acid seawater was caused by the reduced degree of freedom of CO_3^{2-}. The H^+ and Cl^- released from the HCl compound had a chance to simultaneously block CO_3^{2-} interaction with water molecules. The H^+ could be easily interacting with the free oxygen dipole on CO_3^{2-}. The result of this interaction was the H^+ bonding to form C-O-H which slowed down the CO_3^{2-} movement. Whereas the highly electronegative Cl^- was likely to compete with the CO_3^{2-} to reform HCl. The presence of O_2 helped to reduce the competition, specifically the CO_3^{2-} inhibition, as it blocked H^+ movement. The presence of competing ions lowers the oxygen supply due to an imbalance between chemical oxygen demand (COD) and biological oxygen demand (BOD). A higher COD will drop the oxygen supply for BOD [19]. Therefore, the reduced mobility of H^+ can be interpreted as the survivability reduction of the biotic components in the water system.

Further analysis on the results of the shifting pH value in alkaline modified seawater shown in Fig. 1, which subsequently described in Fig. 2, can be conceived as follows. Lennard-Jones potential inferred that the addition of O_2 promoted a stronger interaction between OH^- and CO_3^{2-}. In this case, the OH^- was slightly closer to the buffering CO_3^{2-} ion than O_2. As a result, the CO_3^{2-} repulsed OH^- even stronger, hence the much shorter intramolecular OH^- bond compared to that without O_2. In summary, the robust interaction between CO_3^{2-} and OH^- explained why the pH returns to 9.2 in both with and without aeration.

The shorter bond length of the OH^- (Table 1) implied that the dissolved oxygen repulsed any oxide. There is no

possible way for O_2 to interact with water molecules through electrostatic interaction either by Debye, Keesom, or Van der Waals interaction. However, the nonpolar O_2 molecular orbital vacancy attracted the diamagnetic water molecules. The interaction was possible due to the spin coupling phenomenon. The paramagnetic O_2 spin coupling interaction with bonded hydrogen atom (R–H) in a solvent is well known to energize the reaction [20]. Hence, the repulsion is due to the electrostatic interaction when two or more electrons from O_2 orbital interact with electrons from another molecule orbital.

Furthermore, the results indicated that the atoms of the aerated alkaline modified seawater (Fig. 3, *b*) were forced to vibrate. According to the statistical mechanics point of view, atom vibration within the aerated alkaline seawater system is the indication of its kinetic energy, which also is the representative system entropy [21]. Therefore, the rising energy of the aerated alkaline seawater is the effect of the chaining continuous repulsion. The continuous repulsion was favored by the presence of OH^- in the alkaline condition. The O_2 that temporarily spin coupling with the OH^- was the driver of the continuous molecular movement in the aerated alkaline seawater. This was due to the more mobile and less restrictive OH^- movement compared to the water molecule motion. Therefore, the possibility of OH^- to change its state in each restrictive phase, such as being involved in hydrogen bond or temporary Keesom interaction with water molecule to spin coupling with O_2, was higher. The OH^- could occupy more states than water in the equal period. Consequently, the entropy of the seawater was higher with the addition of bases.

The aeration of the alkaline water increased the entropy even further. The O_2 and OH^- spin coupling could initiate the vibration of a water molecule, which also transferred the vibration to another bonded molecule. The transfer mechanisms were through the weakening of hydrogen bonding and the triggering of dipole induction. The hydrogen bond can possibly be weakened if a water molecule experienced a shear force that depended on the angle of attack of the initiator. Meanwhile, the dipole induction may be triggered due to the direct repulsion by the ions or O_2. It is because the amount of the exerted Coulomb force of a proton largely depends on an atom size, due to the less effective electron shielding when each orbital level has been fully occupied by the electrons [22]. The O_2 was favored by the less effective shielding in influencing water molecule state. Hence, the O_2 and OH^- cooperation was effective to expand the local phenomenon of water vibration globally. Conclusively, the global energy transfer was the main cause of the vibrating system and explained why the alkaline aerated water could be an endothermic system as found in the results.

The mean-field particle simulation was used in the evaluation of the seawater system. This simulation is originally implemented to assess the average behavior of a collective dynamics system [23]. Previous research on the promotion of mitotic spindle bipolarity by mechanical torque considered the mean-field approximation to better understand the cellular biology mechanisms in general [24]. The approximation was thought to be a possible approach as an average of multiple microtubules at work. This is understandable since the involved forces between centrosomes, chromosomes, and microtubules in mitotic spindle covered a large molecular simulation system. However, this mean-field approximation served only as an initial concept to the interacting-particle model that were used along with other models to gain more understanding of the mitotic spindle bipolarity [24].

In our case, the mean-field particle simulation was applied directly with self-propelling algorithm to explain the physicochemical behavior of the seawater system. The analysis results by Mean-field particle and molecular dynamics simulations demonstrated in Fig. 4 is consistent with the gas kinetic theory that presents the kinetic energy of any ideal gas is linearly dependent on the expressed temperature [25]. Therefore, the role of dissolved O_2 will be greater in the higher temperature, but the dissolved O_2 may leave the water system as it is easier to be evaporated.

Some limitations are still imposed on self-propelling algorithms used in the mean-field particle simulation to observe a molecular system. This is because the self-propelling algorithm is originally designed to observe the collective dynamics of a swarm system that consist of moving individuals such as bacteria, protozoa, or swarm robots. The utilization of self-propelling algorithms other than those purposes is reported for the first time in this study. It was implemented to observe a molecular system that naturally can be in a stationary or dynamical state. Hence, in this study, an adjustment was made by assuming that the atoms and molecules movement is like any Newtonian swarm system, which could be a sort of disadvantage. Thus, to further improve the simulation, the integration of quantum mechanics may be considered in the future to simulate the kind of molecular systems as studied in this research, in a more precise manner.

These results may provide a new insight on the importance of aeration in aquaculture. Aeration not only provide sufficient O_2 but also help to stabilize pH to avoid stress, suppress microbial pathogens, and improve the growth performance of the cultured marine organisms. Additionally, by utilizing aeration, the use of chemicals for pH maintenance can be avoided, hence preventing excessive treatment that may harm the surrounding environment. To sum up, these results may serve as a reference for suitable and environmentally friendly treatment in aquaculture maintenance, especially during the events of hypoxia and pH shift.

7. Conclusions

1. The pH of both the aerated acid- and alkaline-modified aquaculture seawater equilibrated faster compared to the non-aerated ones. The pH of the aerated alkaline-modified seawater even moved towards the baseline of 7.00 which ended at 8.7 on day 7. This indicates the role of dissolved oxygen in pH recalibration. To ascertain the role of oxygen, the system was subsequently examined in molecular level.

2. The molecular mechanics analysis of acid-modified seawater demonstrated that the presence of dissolved oxygen reduced the inhibition of the carbonate ion as indicated by 17.71 % shorter OH bond. Meanwhile, in the alkaline modified seawater, the addition of O_2 accelerates the reaction of the existing carbonate buffer system with the surplus ions to recalibrate the pH value.

3. Further self-propelling algorithm and mean-field particle simulation of the alkaline-modified seawater pointed out that the spin coupling phenomenon explained how the dissolved oxygen repulses any oxide. The temporary spin coupling also occurs between oxygen and the OH- atom, which is more mobile than water molecule as numerically

shown by the 1 % O-O bond elongation that followed by 17.71 % shorter O-H bond. As a result, the vibration of carbonate ion due to repulsion with oxygen atoms and the O_2-OH- cooperation promotes global vibrations that increased entropy thus returned the alkaline pH value to the baseline.

Conflict of interest

The authors declare that they have no conflict of interest in relation to this research, whether financial, personal, authorship or otherwise, that could affect the research and its results presented in this paper.

Acknowledgments

The authors are deeply grateful to Yogita A. D. Susanti, Zulkisam Pramudia, Abdul Azis Amin, and Adi Tiya Yanuar from Microbial Resources and Biotechnology research group of the Postgraduate School of Brawijaya University for their assistance.

References

1. Henriksson, P. J. G., Tran, N., Mohan, C. V., Chan, C. Y., Rodriguez, U.-P., Suri, S. et. al. (2017). Indonesian aquaculture futures – Evaluating environmental and socioeconomic potentials and limitations. Journal of Cleaner Production, 162, 1482–1490. doi: https://doi.org/10.1016/j.jclepro.2017.06.133
2. Rimmer, M. A., Larson, S., Lapong, I., Purnomo, A. H., Pong-Masak, P. R., Swanepoel, L., Paul, N. A. (2021). Seaweed Aquaculture in Indonesia Contributes to Social and Economic Aspects of Livelihoods and Community Wellbeing. Sustainability, 13 (19), 10946. doi: https://doi.org/10.3390/su131910946
3. Zhang, P., Zhang, X., Li, J., Huang, G. (2006). The effects of body weight, temperature, salinity, pH, light intensity and feeding condition on lethal DO levels of whiteleg shrimp, Litopenaeus vannamei (Boone, 1931). Aquaculture, 256 (1-4), 579–587. doi: https://doi.org/10.1016/j.aquaculture.2006.02.020
4. Thulasi, D., Muralidhar, M., Saraswathy, R. (2020). Effect of sulphide in Pacific white shrimp Penaeus vannamei under varying oxygen and pH levels. Aquaculture Research, 51 (6), 2389–2399. doi: https://doi.org/10.1111/are.14582
5. Chan, F., Barth, J., Kroeker, K., Lubchenco, J., Menge, B. (2019). The Dynamics and Impact of Ocean Acidification and Hypoxia: Insights from Sustained Investigations in the Northern California Current Large Marine Ecosystem. Oceanography, 32 (3), 62–71. doi: https://doi.org/10.5670/oceanog.2019.312
6. Zeebe, R. E. (2012). History of Seawater Carbonate Chemistry, Atmospheric CO_2, and Ocean Acidification. Annual Review of Earth and Planetary Sciences, 40 (1), 141–165. doi: https://doi.org/10.1146/annurev-earth-042711-105521
7. Anggayasti, W. L., Mancera, R. L., Bottomley, S., Helmerhorst, E. (2017). The self-association of HMGB1 and its possible role in the binding to DNA and cell membrane receptors. FEBS Letters, 591 (2), 282–294. doi: https://doi.org/10.1002/1873-3468.12545
8. Ulaje, S. A., Lluch-Cota, S. E., Sicard, M. T., Ascencio, F., Cruz-Hernández, P., Racotta, I. S., Rojo-Arreola, L. (2020). Litopenaeus vannamei oxygen consumption and HSP gene expression at cyclic conditions of hyperthermia and hypoxia. Journal of Thermal Biology, 92, 102666. doi: https://doi.org/10.1016/j.jtherbio.2020.102666
9. Sultana, T., Haque, M., Salam, M., Alam, M. (2017). Effect of aeration on growth and production of fish in intensive aquaculture system in earthen ponds. Journal of the Bangladesh Agricultural University, 15 (1), 113–122. doi: https://doi.org/10.3329/jbau.v15i1.33536
10. Tanveer, M., Roy, S. M., Vikneswaran, M., Renganathan, P., Balasubramanian, P. (2018). Surface aeration systems for application in aquaculture: A review. International Journal of Fisheries and Aquatic Studies, 6 (5), 342–347. Available at: https://www.fisheriesjournal.com/archives/2018/vol6issue5/PartE/6-5-23-591.pdf
11. Wang, X., Shang, Y., Kong, H., Hu, M., Yang, J., Deng, Y., Wang, Y. (2020). Combined effects of ocean acidification and hypoxia on the early development of the thick shell mussel Mytilus coruscus. Helgoland Marine Research, 74 (1). doi: https://doi.org/10.1186/s10152-020-0535-9
12. Sylvain, F.-É., Cheaib, B., Llewellyn, M., Gabriel Correia, T., Barros Fagundes, D. et. al. (2016). pH drop impacts differentially skin and gut microbiota of the Amazonian fish tambaqui (Colossoma macropomum). Scientific Reports, 6 (1). doi: https://doi.org/10.1038/srep32032
13. George, M. N., Andino, J., Huie, J., Carrington, E. (2019). Microscale pH and Dissolved Oxygen Fluctuations within Mussel Aggregations and Their Implications for Mussel Attachment and Raft Aquaculture. Journal of Shellfish Research, 38 (3), 795. doi: https://doi.org/10.2983/035.038.0329
14. Carstensen, J., Duarte, C. M. (2019). Drivers of pH Variability in Coastal Ecosystems. Environmental Science & Technology, 53 (8), 4020–4029. doi: https://doi.org/10.1021/acs.est.8b03655
15. Hlordzi, V., Kuebutornye, F. K. A., Afriyie, G., Abarike, E. D., Lu, Y., Chi, S., Anokyewaa, M. A. (2020). The use of Bacillus species in maintenance of water quality in aquaculture: A review. Aquaculture Reports, 18, 100503. doi: https://doi.org/10.1016/j.aqrep.2020.100503

16. Irawan, Y., Fonda, H., Sabna, E., Febriani, A. (2021). Intelligent Quality Control of Shrimp Aquaculture Based On Real-Time System and IoT Using Mobile Device. International Journal of Engineering Trends and Technology, 69 (4), 49–56. doi: https://doi.org/10.14445/22315381/ijett-v69i4p208
17. Diez, A. (2021). SiSyPHE: A Python package for the Simulation of Systems of interacting mean-field Particles with High Efficiency. Journal of Open Source Software, 6 (65), 3653. doi: https://doi.org/10.21105/joss.03653
18. D'Orsogna, M. R., Chuang, Y. L., Bertozzi, A. L., Chayes, L. S. (2006). Self-Propelled Particles with Soft-Core Interactions: Patterns, Stability, and Collapse. Physical Review Letters, 96 (10). doi: https://doi.org/10.1103/physrevlett.96.104302
19. Ahmed, A. A. M. (2017). Prediction of dissolved oxygen in Surma River by biochemical oxygen demand and chemical oxygen demand using the artificial neural networks (ANNs). Journal of King Saud University - Engineering Sciences, 29 (2), 151–158. doi: https://doi.org/10.1016/j.jksues.2014.05.001
20. Minaev, B. F. (2017). Spin-orbit coupling mechanism of singlet oxygen a1Δg quenching by solvent vibrations. Chemical Physics, 483-484, 84–95. doi: https://doi.org/10.1016/j.chemphys.2016.11.012
21. Hosoya, A., Maruyama, K., Shikano, Y. (2015). Operational derivation of Boltzmann distribution with Maxwell's demon model. Scientific Reports, 5 (1). doi: https://doi.org/10.1038/srep17011
22. Hua, Z., Tian, C., Qiu, Z., Li, Y., Tian, X., Wang, M., Li, E. (2018). An investigation on NO_2 sensing mechanism and shielding behavior of WO_3 nanosheets. Sensors and Actuators B: Chemical, 259, 250–257. doi: https://doi.org/10.1016/j.snb.2017.12.016
23. Golse, F. (2016). On the Dynamics of Large Particle Systems in the Mean Field Limit. Lecture Notes in Applied Mathematics and Mechanics, 1–144. doi: https://doi.org/10.1007/978-3-319-26883-5_1
24. Miles, C. E., Zhu, J., Mogilner, A. (2022). Mechanical Torque Promotes Bipolarity of the Mitotic Spindle Through Multi-centrosomal Clustering. Bulletin of Mathematical Biology, 84 (2). doi: https://doi.org/10.1007/s11538-021-00985-2
25. Grozdanov, S., Schalm, K., Scopelliti, V. (2019). Kinetic theory for classical and quantum many-body chaos. Physical Review E, 99 (1). doi: https://doi.org/10.1103/physreve.99.012206